Complex wavelet transform: an application to retrieve shear wave splitting time behavior at Mt. Vesuvius

F. Bianco[1], L. Zaccarelli[1, 2], M. Castellano[1] and G. Gargiulo[1]

[1] *Istituto Nazionale di Geofisica e Vulcanologia, Napoli, Italy*
[2] *Institut de Physique du Globe, Paris, France*

(Received: April 8, 2009; accepted: September 15, 2009)

ABSTRACT Shear wave splitting is the elastic equivalent of the well-known phenomenon of optical birefringence. A shear wave, propagating through an anisotropic volume, splits into two *S* waves (qS_1 and qS_2) that travel with different velocities and different polarization directions. This process generates two observables: T_d that is the time delay between the two split *S*-waves, and the polarization direction of the faster one, qS_1. Interpretations indicate that in the upper crust this phenomenon occurs in zones of fluid-filled cracks, microcracks or preferentially oriented pore spaces. The time evolution of the anisotropic distribution of the microcracks due to differential stress according to the nonlinear anisotropic poroelasticity model, is explained by the migration of the fluid along pressure gradients between neighbouring microcracks and pores. In this framework, the shear wave splitting parameters are indicators of the state of stress in the upper crust. We obtained shear wave splitting measurements for local earthquakes occurring before the largest earthquake (M=3.6 occurred on October 9, 1999) recorded at Mt. Vesuvius after the last eruption (March 1944). The arrival times of split shear waves and the polarization directions were detected by using the wavelet transform of a three-component signal. In order to avoid any spatial effects on the time behaviour of the parameters, we performed the analysis for a selected data set of doublets. A short term (of the order of tens of days) variation of both T_d and qS_1 parameters are retrieved before the occurrence of the M=3.6 event.

1. Introduction

Seismic anisotropy is widely observed in the upper crust, regardless of the tectonic setting. This phenomenon has been interpreted as occurring in zones of fluid-filled cracks, microcracks or preferentially oriented pore spaces. The time evolution of the anisotropic distribution of microcracks due to a differential stress, according to the nonlinear anisotropic poroelasticity (APE) model, is explained by the migration of the fluid along pressure gradients between neighbouring microcracks and pores (Crampin and Zatsepin, 1997; Zatsepin and Crampin, 1997). Stress intensity variations cause modifications of the fluid mobility and consequently of the anisotropic characteristics of the medium. In this framework, the shear wave splitting parameters, T_d and qS_1, are indicators of the stress field in the upper crust. Time delay variations are related to changes in microcrack density and the aspect ratio, while the polarization directions of the two *S*-waves interchange (90°-flip) when the system reaches an overpressurized regime [Crampin *et al*. (2004) and references therein]. Previous observations of splitting parameters in several

volcanic environments included Hawaii (Booth *et al*., 1992; Munson *et al*., 1995), and Long Valley Caldera (Savage *et al*., 1990). Changes in shear wave splitting have been observed during the 1989 and the 2001 eruption at Mt. Etna, Sicily (Bianco *et al*., 1998b; Bianco *et al*., 2006), before the 1996 eruption of Mount Ruapehu, New Zealand (Miller and Savage, 2001; Gerst and Savage, 2004); before the 1996 October eruption at Vatnajökull, Iceland (Volti and Crampin, 2003), and before the M=3.6 earthquake at Mt. Vesuvius, October 1999 (Del Pezzo *et al*., 2004). The splitting parameters are measured through a wide variety of approaches such as visual inspection (e.g., Volti and Crampin, 2003), the cross-correlation method (e.g., Savage *et al*., 1989), diagonalization of the covariance matrix (e.g., Cochran *et al*., 2006) and singular value decomposition (Bianco *et al*., 2006). Our main goal is to improve the splitting parameter estimate in semi-automatic algorithms by using the wavelet transform properties to detect both T_d and qS_1 directions. We tested the wavelet-based splitting analysis on families of events that occurred during 1999; we chose this test period since it includes the M=3.6 event that occurred on October 9, 1999, possibly the most energetic one ever recorded after the 1944 eruption.

2. Tectonic setting and seismic network

Mt. Vesuvius is a stratovolcano located in the Campania plain (southern Italy) at the intersection of two main fault systems oriented N-NW - S-SE and N-NE - S-SW (Hyppolite *et al*., 1994). It is formed by an ancient caldera (Mt. Somma) and by a younger volcanic cone (Mt. Vesuvius). Volcanic activity dates back to 300–500 ky [Bianco *et al*. (1998a) and references therein] and is characterized by both effusive and explosive regimes. Three types of regimes of volcanic activity may be identified: large-scale explosive Plinian eruptions, intermediate sub-Plinian eruptions, and small-scale effusive eruptions. The last eruption, in March 1944, was mainly effusive. It may have started a new obstructed conduit phase and hence a quiescent stage. The velocity structure beneath Mt.Vesuvius has been deduced by seismic tomography. Results obtained from the surface down to a depth of 10 km below sea level (b.s.l.) (Zollo *et al*., 1996; Auger *et al*., 2001) suggest the presence of a melting zone at a depth of about 8 km. Scarpa *et al*. (2002) carried out a simultaneous inversion of travel time and hypocentral parameters of the local earthquakes in the same area showing a high-resolution image of the compressional wave velocities for the shallow edifice of Mt. Vesuvius. They showed a high *P*-wave velocity zone, with a rough cylindrical symmetry about the crater axis, extending from the surface down to a depth of approximately 2 km, where it encounters the carbonate basement. Bianco *et al*. (1996) and Del Pezzo *et al*. (2004) put in evidence the presence of an anisotropic volume affecting the upper crust of Mt. Vesuvius, at least in the first 4 km. The seismicity of Mt. Vesuvius has been described in a number of papers [see Scarpa *et al*. (2002) and references therein]. The seismicity appears to extend down to 5 km below the central crater, with most of the energy (up to local magnitude 3.6) clustered in a volume spanning 2 km in depth, positioned at the border between the limestone basement and the volcanic edifice. Quakes are mainly of volcano-tectonic type (VT), with fault-plane orientations showing no regular spatial pattern. During 1999, the seismic monitoring system of Neapolitan volcanoes (Vesuvius, Campi Flegrei, and Ischia Island) was made up of 23 short-period stations telemetered to the acquisition center in Naples and continuously sampled at 100 samples/s. In addition, five 3D stations (Lennartz PCM 5800) were set up in the area of Mt.

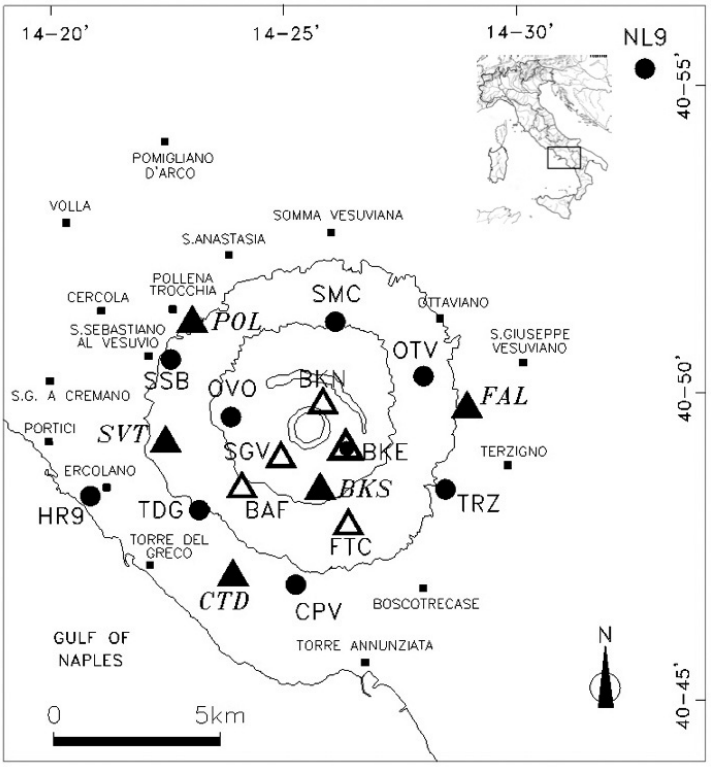

Fig. 1 - The seismic subnet of Mt. Vesuvius. Solid circles represent analogical stations. Triangles (black and white) indicate the position of the temporary digital 3D stations.

Vesuvius from 1997 to the end of 2000. Details of both seismic network configurations and instruments are described in Castellano *et al*. (2002); the subnet of Mt. Vesuvius is depicted in Fig. 1.

3. Methods

When shear waves transmit through a zone of aligned microcracks they split into two components with different velocities and polarizations if the crack size is much smaller than the wavelength. Therefore, if the shear-wave splitting is detected in the same waveforms, there are possibilities of detecting the width and density of the microcrack zone and of estimating the stress direction from the principal direction of the aligned cracks. We used the Wavelet Tranform (hereafter *WT*) to detect the difference in traveltime between two split shear waves, since we expected the arrival time difference to be small. The *WT* is defined as follows (Moriya *et al*., 2006):

$$WT(a,b) = \frac{1}{\sqrt{a}} \int_{-\infty}^{\infty} x(t) h^*\left(\frac{t-b}{a}\right) dt \qquad (1)$$

where *x(t)* is the signal to be analyzed and *h (a, t - b)* is the kernel. The symbol * denotes the

complex conjugate. The kernel generally assumes the following form:

$$h(a,t-b) = e^{-\frac{1}{2}(\frac{t-b}{a})} e^{j\omega_0(\frac{t-b}{a})} \tag{2}$$

where a and b are called 'scale' and 'shift', respectively and ω_0 is the central frequency.

To detect the phase alignment, we used a 'phase alignment index' (*PAI*) defined as:

$$PAI\ (b) = Re[\xi\ (b)], \tag{3}$$

where:

$$\xi(b) = e^{-jb} \int_0^\infty e^{-j\arg(WT)} \omega(a) da \tag{4}$$

and *arg(WT)* is the phase of the complex function *WT(a,b)* of the signal and $\omega(a)$ satisfies the following normalization:

$$\int_0^\infty \omega(a) da = 1. \tag{5}$$

For the multiplets recorded at Mt. Vesuvius, we constructed the kernel by means of the Morlet wavelet defined as:

$$\Psi(a,t) = e^{-(\frac{t}{a})^2} e^{\frac{-j\omega t}{a}} \tag{6}$$

satisfying the following spatial localization condition:

$$\int_{-\infty}^\infty \Psi(t) dt = 0. \tag{7}$$

4. Data

First, we used the following criteria for a rigorous selection of the seismic records: i) clear shear wave onsets with high Signal-to-Noise ratios: S/N > 6; and ii) incidence angles strictly inside the shear wave window (theoretically 35°) to ensure there was no interaction with the free surface. To obtain the S/N ratio, we measured the noise amplitude for all three-components before the *P*-wave onset. Only the data from the Lennartz 5800 digital 3-D stations (Fig. 1; 125 s.p.s. reaching a dynamic range of 120 dB by means of a gain ranging amplifier) passed our selection

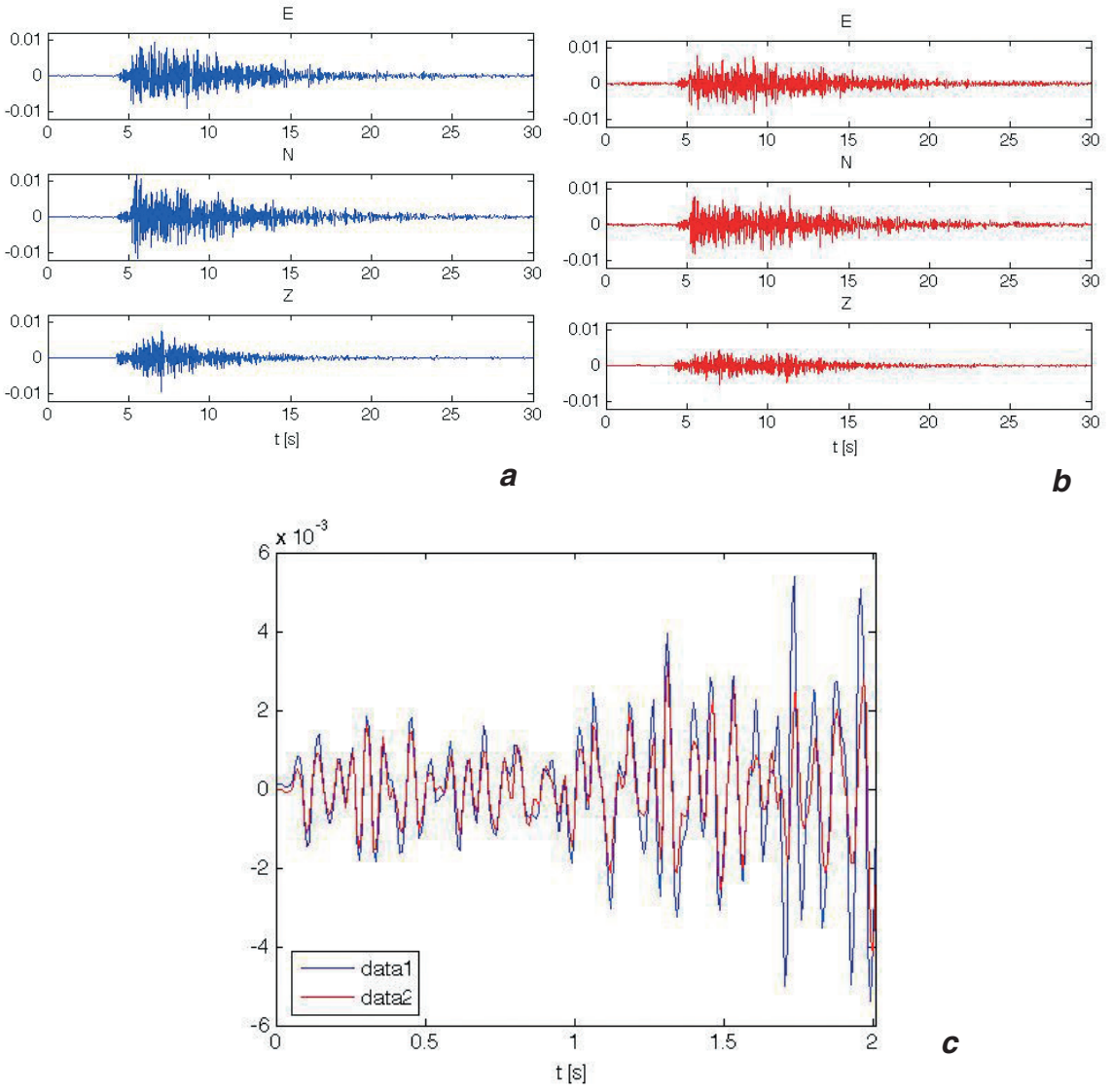

Fig. 2 - An example of doublet recorded at the BKN station: a) event occurred on 1999/11/27 (data1); b) event occurred on 1999/12/21 (data2); c) comparison of the vertical components of data1 and data2.

rules, and hence were used for the shear wave splitting analysis. The signals are not clipped in the *S*-wave time window, even for the largest magnitude event. Families of repeating, almost identical earthquakes or multiplets exist among the VT-events recorded by all the network (Fig. 1). The similarity of repeating events, recorded at the same station, indicates that the source and wave paths are almost the same (Geller and Mueller, 1980). To reduce the mixing of spatial and temporal effects in the data, we searched for similar events among those that passed the previous selection; similar events were identified by performing cross-correlation calculations (Aster and Scott, 1993) for all the event pairs with hypocentral separations less/equal the location error. We

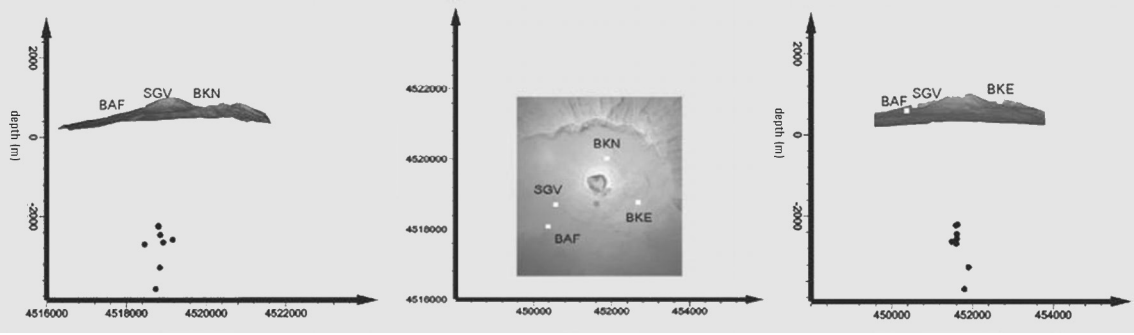

Fig. 3 - Location of the selected doublets/multiplets. Coordinates are UTM.

consider "similar" those events exhibiting a normalized cross-correlation factor cc≥0.9 calculated on a time signal window starting at the *P* onset and ending 1 s after. In this way, we identified one multiplet and 3 doublets, spanning June to December 1999. The above-selected events were recorded by BAF, BKE, BKN and SGV stations, and all, exhibited incidence angles in the range 16° - 35°. In Fig. 2, an example of a doublet recorded at the BKN station is reported. The selected doublets/multiplets inside the shear wave windows are located in the crater area in the first 2 - 3 km of the upper crust (Fig. 3), which is inside the usual seismogenetic volume of Mt. Vesuvius (e.g., Scarpa *et al*., 2002). Please note that to locate the events we used the records of the entire network (see Fig. 1).

5. Results

On the data rotated clockwise 2°step by 2°step (in the range 0-180°) we applied, at each step, the *WT* using four different wavelets with ω equal to 2, 5, 50 and 250, respectively. Then we search for the maximum value of the following

$$MP = \frac{1}{K}\sum_i PAI_i \qquad (8)$$

where K is the number of wavelets used (in our case K=4). In order to obtain an estimate of both splitting parameters, for each event, at each station, we computed the *MP* distribution of Eq. (8), as function of both the rotation angle and the time, obtaining the representation in Fig. 4. The time lag between the first two maxima (the red zones) is a measure of the splitting parameter T_d, and the rotation angle corresponding to the first maximum is a measure of the splitting parameter qS_1. In this way, we obtained our splitting measurements for the doublets/multiplets recorded at each station. Finally, we corrected the T_d measurements for the raypath length, defining the normalized time delay $T_n = T_d/D$ where D is the hypocentral distance of the event. From the splitting parameter estimates, we were able to infer their time behaviour at each station, as shown in Figs. 5 and 6. At stations BKE and SGV, we observed an increase of T_n followed by a sudden decrease

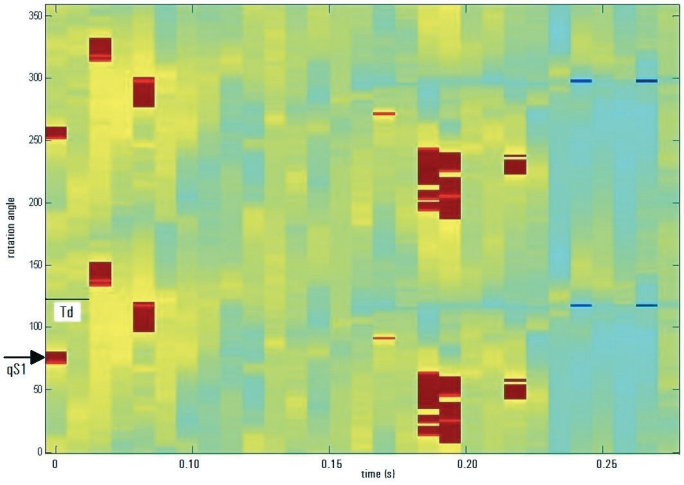

Fig. 4 - Distribution of the phase index (*PAI* function) as a function of the rotation angle θ and time.

just before the occurrence of the *M*=3.6 event (Fig. 5). A compatible behaviour is observed at the BKN station, whilst at the BAF station the unique doublet shows a decrease of T_n after the occurrence of the *M*=3.6 event (Fig. 5). The temporal pattern of the polarization directions for the fast split shear wave at each station is represented in the plots of Fig. 6. The time pattern at all the stations shows variations in time sometimes of 90°, before the occurrence time of the *M*=3.6 event.

6. Discussion and conclusions

Through the *WT* features, we obtained estimates of the splitting parameters for a sequence of doublets/multiplets in a time window including the occurrence of the most energetic event recorded at Mt. Vesuvius since the end of the last eruption (March 1944). The selected data had incidence inside the shear wave window (35°), avoiding any misinterpretation due to the free surface interaction of the *S* wave-field. Using wavelets, we preserved the signal signature, realizing a fast algorithm easily implemented in the semi-automated codes. We tested this approach on data collected at Mt. Vesuvius, where the presence, in the upper crust of anisotropy due to fluid-filled, stress aligned microcracks (EDA cracks), is well established (i.e., Bianco *et al*., 1999; Del Pezzo *et al*., 2004; Bianco and Zaccarelli, 2009). We routinely investigated the dependence of both splitting parameters on backazimuth, focal mechanisms and initial polarization, excluding the fact that the retrieved measures are dependent on this factor. Moreover, by comparing pairs of seismograms from doublets or multiplets, we investigated temporal variations in the propagation properties of the medium, discovering changes in the splitting parameters behaviour that are, possibly, related to the stress field variation due to the occurrence of the *M*=3.6 event. In particular, we observed an increase of the normalized time delay, starting approximately 3 months before the occurrence of the *M*=3.6 event, followed by a sudden decrease, roughly 20 days before the occurrence of the *M*=3.6 event (Fig. 5). Also, the polarization of the fast *S* wave shows a variation, sometimes exhibiting a 90°-flip before the

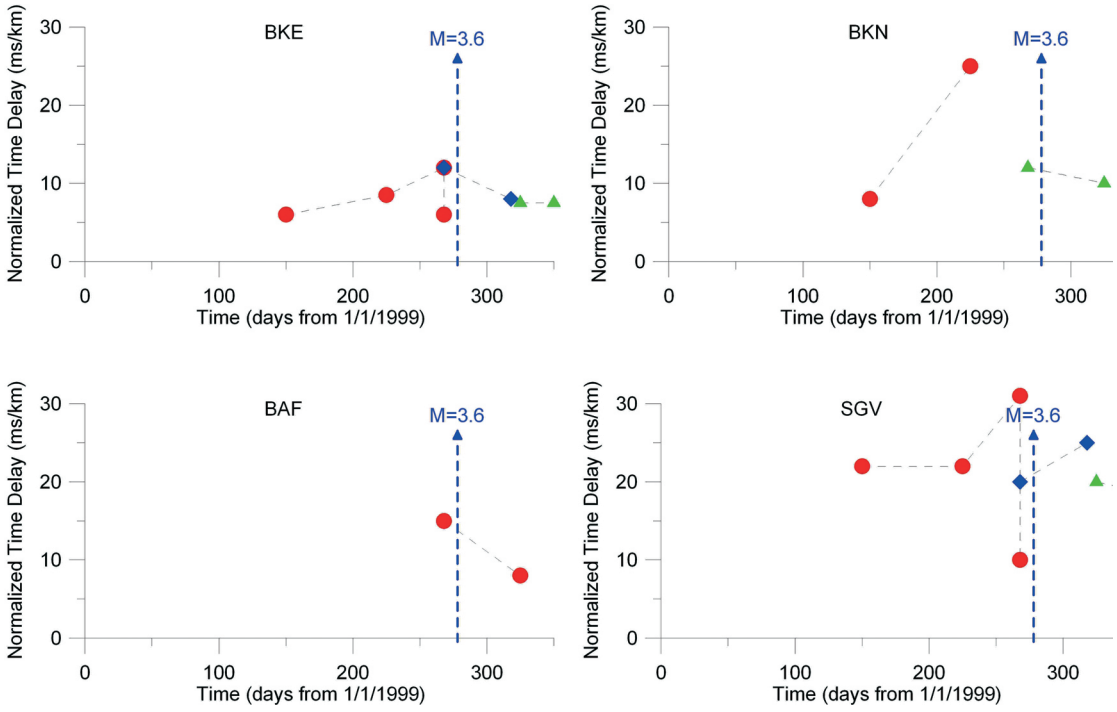

Fig. 5 - Time pattern of the normalized time delay at stations BKE, BKN, BAF and SGV. Each doublet/multiplet is marked by a different symbol. The vertical arrow points towards the time (October 9, 1999) of occurrence of the M=3.6 events. The dashed line connects the events belonging to the same doublet/multiplet.

October 9 event (Fig. 6). An increase of the time delay along ray paths in the doubleleafed solid angle of directions 16°-35° corresponds, according to the APE modelling, to an increase in the aspect-ratio of the EDA cracks. Similar increases have been observed worldwide before certain earthquakes (Crampin *et al*., 1990, 1991; Gao *et al*., 1998; Volti and Crampin, 2003; Gao and Crampin 2004; and elsewhere). The APE modelling suggests (Crampin and Zatsepin, 1997; Crampin, 1999) that the observed long-term increase of T_d is monitoring the effects of the accumulation of stress as a modification to microcrack geometry. The accumulation of stress continues until a certain level of cracking, referred to as fracture criticality, is reached when the rocks are so fractured that they reach the percolation threshold and the rock fractures (Crampin, 1993). Thus the increase in time delays in Fig. 5 may be interpreted as monitoring stress accumulation before the main energetic rupture occurs. Similarly, decreases in the average T_d immediately before the M=3.6 are also observed immediately before earthquakes [whenever there are sufficient observations immediately before the event to display the phenomenon: Gao and Crampin (2004)]. These decreases are interpreted as a stress relaxation caused by crack coalescence, as the fault plane approaches the onset of fracturing. The APE modelling suggests that when increasing pore-fluid pressures reach critically high levels (as they do on all seismically active faults), the effective stress-field realigns microcrack distributions, and causes 90°-flips in

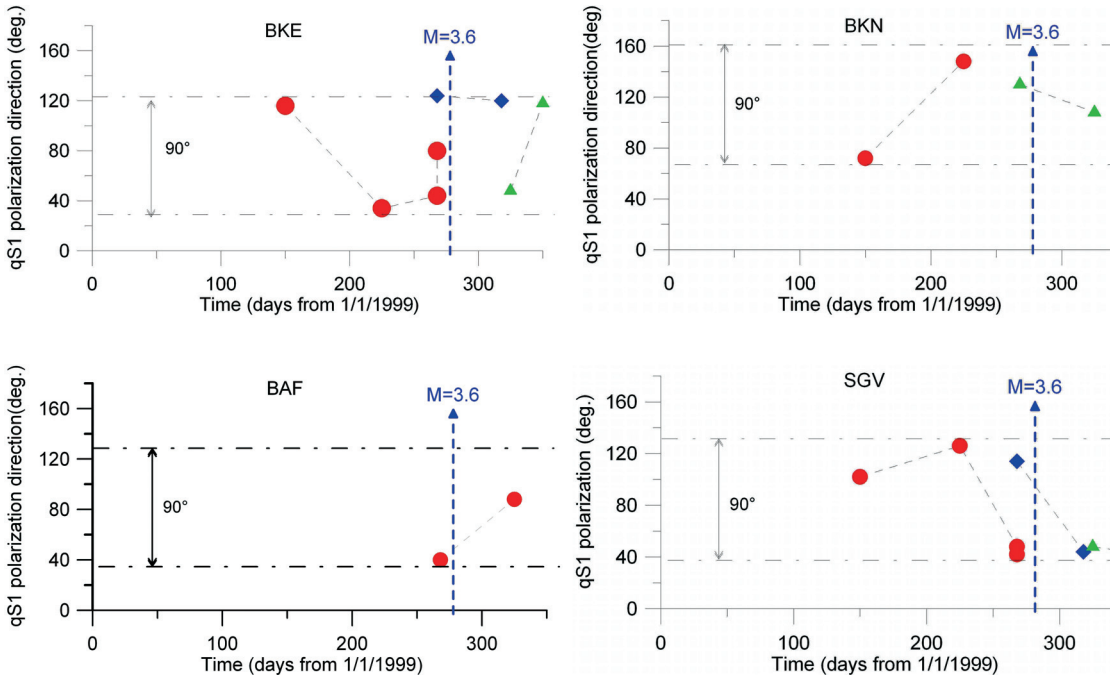

Fig. 6 - Time pattern of the qS_1 polarization direction at stations BKE, BKN, BAF and SGV. Each doublet/multiplet is marked by a different symbol. The vertical arrow points towards the time (October 9, 1999) of occurrence of the M=3.6 events. The dashed line connects the events belonging to the same doublet/multiplet; the horizontal dashed-dotted lines highlight the 90°-flip.

shear wave polarizations [Crampin *et al*. (2004) and references therein]. Before the M=3.6, we observed a change of 90° for the qS_1 polarization (for events belonging to the same family) at BKE (approximately 2 months before), at BKN (approximately 1 month before) and at SGV (approximately 10 days before). The 90°-flip may be the effect of increasing pressure as the main rupture approaches the surface. This reorganizes the local microcrack geometry and causes 90°-flips in the qS_1 polarization even though the reason why this effect seems to be delayed at the different stations is unclear. It has to be clarified that, in the APE framework, the pore pressure and the fluid flux are not involved as individual parameters, whilst only their dimensionless increase and/or decrease are taken into account [Crampin and Zatsepin (1997); Zatsepin and Crampin (1997); Crampin (1999) and references therein]. The fluid-assisted chemical reaction and the effects on the hydraulic regimes, as well as the effects of thermal pressurization of pore waters, are all very important phenomena but, at the spatial scale of our observations and using our seismological approach, they cannot be discussed.

Using a different methodology on a wider set of non-doublet (and non-multiplet too) events, Del Pezzo *et al*. (2004) found time variations of the splitting parameters in correspondence with the M=3.6 occurrence. Our results agree with those retrieved by Del Pezzo *et al*. (2004),

suggesting that a poor (in number) set of doublets/multiplets analyzed with appropriate techniques, allows the reconstruction of a useful time pattern for the splitting parameters. Interestingly, Pandolfi *et al*. (2006), studying the Coda Wave Interferometry for a data set including the one used in the present paper, showed a velocity variation occurring at the same time as the T_d changes; this suggests that coda wave interferometry and shear wave splitting phenomena are sensitive to even small stress field variations, confirming their role as indicators of the state of crustal stress, in time.

REFERENCES

Aster R. and Scott J.; 1993: *Comprehensive identification of similar earthquakes in microearthquake data sets.* Bull. Seism. Soc. Am., **83**, 1307-1314.

Auger E., Gasparini P., Virieux J. and Zollo A.; 2001: *Seismic evidence of an extended magmatic sill under Mt. Vesuvius*. Science, **294**, 1510–1512.

Bianco F. and Zaccarelli L.; 2009: *A reappraisal of shear wave splitting parameters from Italian active volcanic areas through a semiautomatic algorithm*. J. Seism., **13**, 253–266, doi: 10.1007/s10950-008-9125-z.

Bianco F., Castellano M., Milano G. and Vilardo G.; 1996: *Shear-wave polarization alignment on the eastern flank of Mt. Etna volcano (Sicily, Italy).* Annali di Geofisica, **49**, 429–443.

Bianco F., Castellano M., Milano G., Ventura G. and Vilardo G.; 1998a: *The Somma-Vesuvius stress-field induced by regional tectonic: evidences from seismological and mesostructural data*. J. Vol. Geoth. Res., **82**, 199–218.

Bianco F., Castellano M. and Ventura G.; 1998b: *Structural and seismological features of the 1989 syn-eruptive NNW–SSE fractures system at Mt. Etna.* Geoph. Res. Lett., **25**, 1545–1548.

Bianco F., Castellano M., Milano G., Vilardo G., Ferrucci F. and Gresta S.; 1999: *The seismic crisis at Mt. Vesuvius during 1995 and 1996.* Phys. Chem. Earth., **24**, 977–983.

Bianco F., Scarfì L., Del Pezzo E. and Patanè D.; 2006: *Shear wave splitting changes associated with the 2001 volcanic eruption on Mount Etna.* Geophys. Journ. Int., **167**, 959-967, doi:10.1111/j.1365-246X.2006.03152.x

Booth D.C., Wyss M. and Gillard D.; 1992: *Shear-wave polarization alignments recorded above the Kaoiki fault zone, Hawaii.* Geophys. Res. Lett., **19**, 1141–1144.

Castellano M., Buonocunto C., Capello M. and La Rocca M.; 2002: *Seismic surveillance of active volcanoes: the Osservatorio Vesuviano Seismic Network (OVSN– southern Italy).* Seim. Res. Lett., **73**, 168–175.

Cochran E.S., Li Y.G. and Vidale J.E.; 2006: *Anisotropy in the shallow crust observed around the San Andreas Fault before and after the 2004 M 6.0 Parkfield earthquake*. Bull. Seism. Soc. Am., **96**, 364-375, doi: 10.1785/0120050804.

Crampin S.; 1993: *A review of the effects of crack geometry on wave propagation through aligned cracks*. Can. J. Expl. Geophys., **29**, 3-17.

Crampin S.; 1999: *Calculable fluid–rock interactions.* J. Geol. Soc. London, **156**, 501– 514.

Crampin S. and Zatsepin S.V.; 1997: *Modeling the compliance of crustal rock-II. Response to temporal changes before earthquakes.* Geophys. J. Int., **129**, 495–506.

Crampin S., Booth D.C., Evans R., Peacock S. and Fletcher J.B.; 1990: *Changes in shear wave splitting at Anza near the time of the North Palm Springs earthquake.* J. Geophys. Res., **95**, 11197-11212.

Crampin S., Booth D.C., Evans R., Peacock S. and Fletcher J.B.; 1991: *Comment on "Quantitative measurements of shear wave polarizations at the Anza Seismic Network, Southern California: implications for shear wave splitting and earthquake prediction"* by R.C. Aster, P.M. Shearer and J. Berger, J. Geophys. Res., **96**, 6403-6414.

Crampin S., Peacock S., Gao Y. and Chastin S.; 2004: *The scatter of time-delays in shear-wave splitting above small earthquakes.* Geophys. J. Int., **156**, 39–44.

Del Pezzo E., Bianco F., Petrosino S. and Saccorotti G.; 2004: *Changes in coda decay rate and shear-wave splitting parameters associated with seismic swarms at Mt. Vesuvius, Italy*. Bull. Seism. Soc. Am., **94**, 439–452.

Gao Y. and Crampin S.; 2004: *Observations of stress relaxation before earthquakes*. Geophys. J. Int., **157**, 578-582.

Gao Y., Wang P., Zheng S., Wang M., Chen Y. and Zhou H.; 1998: *Temporal changes in shear-wave splitting at an isolated swarm of small earthquakes in 1992 near Dongfang, Hainan Island, southern China.* Geophys. J. Int., **135**, 102–112.

Geller R.J. and Mueller C.S.; 1980: *Four similar events in central California*. Geophys. Res. Lett., **7**, 821-824.

Gerst A. and Savage M.K.; 2004: *Seismic anisotropy beneath Ruapehu volcano: a possible forecasting tool.* Science, **306**, 1543–1547.

Hyppolite J., Angelier J. and Roure F.; 1994: *A major change revealed by Quaternary stress patterns in the southern Apennines.* Tectonophysics, **230**, 199–210.

Moriya H., Tanaka K. and Niituma H.; 2006: *Shear wave splitting detected by using downhole triaxial seismic detector during dilatation of artificial subsurface fracture.* Geophys. J. Int., **164**, 401-410.

Miller V. and Savage M.K.; 2001: *Changes in seismic anisotropy after volcanic eruptions: evidence from Ruapehu.* Science, **293**, 2231–2233.

Munson C.G., Thurber C.H., Li Y. and Okubo P.G.; 1995: *Crustal shear wave anisotropy in southern Hawaii: Spatial and temporal analysis.* J. Geophys. Res., **100**, 20367–20377.

Pandolfi D., Bean C. and Saccorotti G.; 2006: *Coda wave interferometric detection of seismic velocity changes associated with the 1999 M=3.6 event at Mt. Vesuvius.* Geophys. Res. Lett., **33**, L06306. doi:10.1029/2005GL025355.

Savage M.K., Shih X.R., Meyer R.C. and Aster R.C.; 1989: *Shear-wave anisotropy of active tectonic regions via automated S-wave polarization analysis.* Tectonophysics, **165**, 279–292.

Savage M.K., Peppin W.A. and Vetter U.R.; 1990: *Shear wave anisotropy and stress direction in and near Long Valley caldera, California, 1979–1988.* J. Geophys. Res., **95**, 11165–11177.

Scarpa R., Tronca F., Bianco F. and Del Pezzo E.; 2002: *High resolution velocity structure beneath Mt. Vesuvius from seismic array data.* Geophys. Res. Lett., **29**, 2040-2044, doi: 10029/2002GL015576.

Volti T. and Crampin S.; 2003: *A four-year study of shear-wave splitting in Iceland: 2-Temporal changes before earthquakes and volcanic eruptions.* In: Nieuwland R. (ed), New insights into structural interpretation and modeling, Geol. Soc., London, Special publication, 212, pp. 135–149.

Zatsepin S.V. and Crampin S.; 1997: *Modeling the compliance of crustal rock - I. Response of shear-wave splitting to differential stress.* Geophys. J. Int., **129**, 477–494.

Zollo A., Gasparini P., Vireux J., Le Meur H., De Natale G., Biella G., Boschi E., Capuano P., De Franco R., Dell'Aversana P., De Matteis R., Guerra I., Iannacone G., Mirabile L. and Vilardo G.; 1996: *Seismic evidence for a low-velocity zone in the upper crust beneath Mt.Vesuvius.* Science, **274**, 592-594.

Corresponding author: Francesca Bianco
Istituto Nazionale di Geofisica e Vulcanologia, Osservatorio Vesuviano
Via Diocleziano 328, 80124 Napoli, Italy
phone: +39 081 6108328; fax: +39 081 6108351; e-mail: bianco@ov.ingv.it